This is a preprint version of the paper published in Matrix Biol. 2017 Nov;63:55-68.
doi: 10.1016/j.matbio.2016.12.008.
© 2017 Elsevier. This manuscript version is made available under the CC-BY-NC-ND 4.0 license

Hyaluronic acid decreases the mechanical stability, but increases the lytic resistance of fibrin matrices

Running title: Differential effects of hyaluronan on the viscoelasticity and lysibility of fibrin

Erzsébet Komorowicz[a], Nóra Balázs[a], Zoltán Varga[b], László Szabó[c], Attila Bóta[b], Krasimir Kolev[a]

[a]*Department of Medical Biochemistry, Semmelweis University, 1094 Budapest, Tűzoltó utca 37-47., Hungary*

[b]*Department of Biological Nanochemistry, Institute of Materials and Environmental Chemistry, Research Centre for Natural Sciences, Hungarian Academy of Sciences, 1117 Budapest, Magyar Tudósok körútja 2, Hungary*

[c]*Department of Functional and Structural Materials, Institute of Materials and Environmental Chemistry, Research Centre for Natural Sciences, Hungarian Academy of Sciences, 1117 Budapest, Magyar Tudósok körútja 2, Hungary*

Correspondence: Krasimir Kolev, Semmelweis University, Department of Medical Biochemistry, 1094 Budapest, Tűzoltó utca 37-47., Hungary, tel.: +36 1 4591500/60035, fax: +36 1 2670031, e-mail: Krasimir.Kolev@eok.sote.hu

This is a preprint version of the paper published in Matrix Biol. 2017 Nov;63:55-68.
doi: 10.1016/j.matbio.2016.12.008.
© 2017 Elsevier. This manuscript version is made available under the CC-BY-NC-ND 4.0 license

Abstract

Hyaluronic acid (HA) is a large, non-sulfated glucosaminoglycan abundantly present at sites where fibrin is also formed (during wound healing, in arterial restenotic lesions and eroded atherosclerotic plaques). The aim of the present study was to characterize the structure of composite fibrin-HA clots with scanning electron microscopy (SEM), pressure-driven permeation and small-angle X-ray scattering (SAXS) and their viscoelastic properties with an oscillation rheometer. In addition the efficiency of fibrinolysis in these clots was investigated by kinetic turbidimetric and chromogenic assays for dissolution of fibrin and plasminogen activation by tissue-type plasminogen activator (tPA). Fibrin formed in the presence of native (1,500 kDa) HA and its 500 kDa fragments had thicker fibers and larger pores according to the SEM and clot permeation data, whereas the 25 kDa HA fragments had only minor effects. SAXS evidenced a mild disarrangement of protofibrils. These structural alterations suggest that HA modifies the pattern of fibrin polymerization favouring lateral association of protofibrils over formation of branching points. Rheometer data showed softer fibrin structures formed with 1,500 kDa and 500 kDa HA and these clots presented with lower dynamic viscosity values and lower critical stress values at gel/fluid transition. tPA-catalyzed plasminogen activation was markedly inhibited by HA, both in free solution and on the surface of fibrin clots, in the presence and in the absence of 6-aminohexanoate suggesting a kringle-independent mechanism. HA of 1,500 and 500 kDa size prolonged clot lysis with both plasmin and tPA and this inhibition was kringle-mediated, because it was abolished by 6-aminohexanoate abolished and was not observed with des-(kringle1-4)-plasmin. Our data suggest that HA size-dependently modifies the pattern of fibrin polymerization with consequent inhibition of fibrinolysis. At sites of tissue injury and inflammation, HA could stabilize fibrin through modification of its structure and lysibility.

Highlights

- Hyaluronic acid (HA) is enriched in both healthy and atherosclerotic arterial wall.
- Modulation of fibrin(olysis) by HA of varying molecular size is studied.
- Incorporation of large HA results in thicker fibrin fibers enclosing larger pores.
- The HA-modified fibrin structure is less rigid and more susceptible to deformation.
- HA inhibits plasminogen activation by tPA and plasmin-catalysed fibrin degradation.

Keywords: fibrin, fibrinolysis, hyaluronic acid, plasmin, plasminogen activation

This is a preprint version of the paper published in Matrix Biol. 2017 Nov;63:55-68.
doi: 10.1016/j.matbio.2016.12.008.
© 2017 Elsevier. This manuscript version is made available under the CC-BY-NC-ND 4.0 license

1. Introduction

Thrombin, a serine-protease activated in the blood coagulation cascade converts fibrinogen, a rod-shaped soluble plasma protein of 340 kDa to insoluble fibrin polymer [1]. This 3-dimensional fibrin structure provides a solid scaffold in haemostatic and thrombotic clots, and functions as the primary matrix in the wound healing process [2]. Several factors modulate the structure and function of the fibrin network, including thrombin, chloride and calcium concentrations, as well as additional clot components and cellular interactions [3-5]. Fibrin fiber thickness, branching density and porosity of patients' plasma clots have been linked to the frequency of cardiovascular events and thrombolytic resistance [6]. The lytic susceptibility of blood clots may also be related to microembolization, a common event after acute myocardial infarction [7]. Recently we have described that certain extracellular matrix components of the atherosclerotic plaque (chondroitin-sulfate, dermatan-sulfate and decorin) decrease the mechanical and fibrinolytic resilience of the fibrin structure [8]. Hyaluronic acid (HA), a large, non-sulfated glycosaminoglycan is ubiquitously present in extracellular matrices, and appreciated as an important player in wound healing, vascular disease and cancer, where fibrin deposition also occurs [9,10]. HA is found at high concentrations in articular joint synovial fluid (2-3 g/l), human umbilical cord, and the vitrous body of the eye, but its circulating plasma concentration is very low (0.01-0.1 mg/l) [11]. Among human solid tissues, articular cartilage contains 0.5-2.5 g/l, and skin up to 0.5 g/l HA, other organs have less. Plasma HA concentration rises in certain diseases (and may be utilized in diagnostic tests), but the reported values vary over a broad range up to 0.2 g/l in rheumatoid arthritis. Microenvironments of many solid tumours have been found to be rich in HA, and HA content has been linked to poor outcome in cancer patients [9, 11]. In healthy arterial wall it is localized in the endothelial glycocalix, the intima and the adventitia, while in atherosclerotic vessels restenotic lesions and eroded plaques have been found rich in HA [11-13]. Vascular HA has been suggested to play a dual role: in the endothelial glycocalix it may protect endothelial integrity, whereas HA in plaques could promote cell proliferation and neointimal expansion [14]. In advanced atherosclerotic lesions, hyaluronic acid co-localizes with versican, a prothrombotic vascular proteoglycan, and platelets can adhere to HA with specific CD44 receptors, hence versican-HA complexes could serve as platelet adhesion targets at the plaque/thrombus interface [13]. Together with fibrin, HA is also a major component of the primary matrix formed following tissue injury [10]. High-molecular weight HA (over 10^6 Da, "native" HA) released from cells becomes fragmented by hyaluronidase enzymes, as well as by reactive oxygen species at sites of tissue injury and inflammation, leading to a set of HA fragments of highly variable chain length. HA size-variants have been shown to display varying, sometimes even opposing effects on the immune system, angiogenesis and tumour biology. Thus, native HA is anti-inflammatory and anti-angiogenic, while smaller HA fragments promote inflammatory reactions, and angiogenesis, which are crucial events in wound healing and tissue remodelling, as well as in cancer progression [9,10,16]. Despite some early data on the specific binding of human fibrinogen to HA, little is known on the potential role of HA in modulating the formation and behaviour of the fibrin matrix, and no data are available on the size-dependency of these effects [17,18].

We aimed to characterize the HA effects on fibrin structure, and also describe the composite HA/fibrin matrices as a cofactor and substrate for the fibrinolytic system. Fibrinolysis is largely based on a serine-protease, plasmin, formed from its zymogen, plasminogen by plasminogen activators [19,20]. Fibrin has been shown to accelerate tissue plasminogen activator (tPA) mediated plasminogen activation, a phenomenon dependent on fibrin network characteristics [21,22]. Once formed on fibrin, plasmin would proteolytically dissect fibrin fibers leading to the formation of water-soluble fibrin degradation products, but the rate of fibrin degradation also depends on clot structure. Among serine-proteases, plasmin displays special lysine-binding sites located on 5 kringle domains, which play multiple regulatory roles in fibrinolysis. Miniplasminogen lacking the first 4 kringle domains is formed from plasminogen by elastase released from activated neutrophil leukocytes [23,24]. Hence, miniplasmin is not only a useful tool to identify a role for kringle domains in the

This is a preprint version of the paper published in Matrix Biol. 2017 Nov;63:55-68.
doi: 10.1016/j.matbio.2016.12.008.
© 2017 Elsevier. This manuscript version is made available under the CC-BY-NC-ND 4.0 license

regulation of fibrinolysis by HA, but may also be an active plasmin variant at sites of tissue injury and inflammation.

2. Results

Fibrin clots containing various HA size-variants displayed significant changes in their formation, network structure and mechanical properties, as evidenced by several independent methods (Table 1). At HA concentrations of about 1/10 of the fibrin concentration we found significant differences in the examined parameters by all methods, although fibrin fiber thickening by SEM was observable in the presence of native HA at concentration as low as 0.05 g/l and HA effects did not level off even at higher (up to 1 g/l) concentrations. According to the *turbidimetric* clotting assay, the high molecular-weight (1500 kDa and 500 kDa) HA variants delayed the assembly of composite clots, and resulted in higher maximal turbidity values which reflects elevated mass-length ratio of the fibrin fibers [3]. By *morphometric analysis of SEM* images of pure fibrin, and fibrin containing 0.2 g/l HA variants, we found about 15 % relative increase in fibrin fiber diameter in the presence of the high molecular-weight (1500 and 500 kDa) HA molecules, whereas about 5 % thinner fibers were formed when 25 kDa HA fragments were added (representative images are presented in Fig. 1). According to *SAXS* studies, the presence of HA up to 1 g/l in fibrin did not alter the longitudinal periodicity of the end-to-end junctions of fibrin monomers (the sharp peak at 22.2 nm in Fig. 2), nor did it change the average lateral distance between protofibrils in the fibrin network (the broad peak between 4 and 10 nm in Fig. 2) [24,25]. Only the largest, native HA at 1 g/l concentration resulted in a mild disarrangement of protofibrils, reflected by a decrease of the peak between 12.5 and 31 nm, a peak in pure fibrin which is attributed to the presence of a typical cluster unit cell size occurring in fibrin fibers at a high degree of periodicity [25,26]. The relative increase in the sharp peak corresponding to 22.2 nm periodicity is an apparent consequence of the decrease in the broad peak at 12.5-31 nm, on which the sharp peak is normally superimposed. *Clot porosity* was examined by fluid permeability measurements, which indicated a 60 % increase in the Darcy constants in the presence of native and 500 kDa HA, and a much smaller, but statistically significant increase due to the 25 kDa HA fragments. The *viscoelastic properties* of the composite fibrin clots were evaluated with rheological measurements (Fig. 3, Table 1). The course of storage and loss moduli changes during fibrin/HA clot formation indicated a lag-phase in the presence of HA additives, regardless of their size. None of the HA additives influenced the amidolytic activity of thrombin on synthetic, short peptide substrates (data not shown). At the end of the clotting phase, both G' and G'' stabilized at significantly lower values in the case of high molecular weight HAs, whereas the smallest HA fragments did not cause any statistically significant changes. High molecular-weight HAs in fibrin also increased the loss tangent (G''/G'), which indicates an increased energy loss during deformation due to structural rearrangements in fibrin. The flow-curves illustrated in Fig. 3B evidence that the softer clot structures with 1500 kDa and 500 kDa HA additives presented with lower dynamic viscosity values throughout the experiment, and gel/fluid transition occurred at lower critical stress values (τ_0) (Table 1). Considering all of our data on composite fibrin/HA structure, a coarser fibrin network of thicker fibers and larger pores was formed over a longer clotting time in the presence of large (1500 kDa, 500 kDa) HAs, which was softer, suffered more rearrangements upon deformation, and lost its gel state at lower stress.

Further experiments were designed to explore the susceptibility of composite fibrin/HA clots to solubilization by the plasminogen/plasmin system. At first, we addressed the effects of HAs on the *activation of plasminogen by tPA*. tPA-mediated plasminogen activation was markedly inhibited by all HA size-variants, maximal inhibitory effects were observed at concentrations as low as 0.05 g/L (Fig. 4A and Table 2). The inhibitory effect of HA did not change in the presence of 0.5 mM 6-aminohexanoate, which could interfere with high-affinity lysine-binding sites located on plasminogen kringle domains (Fig. 4A). The amidolytic activities of tPA and plasmin on specific synthetic peptide substrates (Spectrozyme-tPA and Spectrozyme-PL, respectively) were not

This is a preprint version of the paper published in Matrix Biol. 2017 Nov;63:55-68.
doi: 10.1016/j.matbio.2016.12.008.
© 2017 Elsevier. This manuscript version is made available under the CC-BY-NC-ND 4.0 license

influenced by the presence of HA additives (not shown). Cyanogenbromide-cleavage products of fibrinogen (FgDP), a cofactor for tPA-mediated plasminogen activation, accelerated plasminogen activation in our model, and in their presence higher (500 μg/ml) concentrations of native HA were necessary to reach a relative inhibition equivalent to the effect of 50 μg/ml HA in the absence of FgDP (Fig. 4A, Inset).

Since plasminogen activation *in vivo* takes place mostly on the surface of fibrin, we also measured *tPA-mediated plasminogen activation on the surface of preformed clots* containing various HA additives. Plasminogen activation rates were significantly lower on the surfaces of composite clots with incorporated HA, and the effects of HA were not size-dependent (Table 2). Since the presence of large HA variants resulted in thickening of fibrin fibers, and coarse fibrin networks have been shown to be worse cofactors [21], we also used low NaCl concentration as a tool to prepare coarse, but pure fibrin clots to compare their effects on plasminogen activation with that of coarse, but composite (with HA) clots. Coarse networks present in general with higher turbidity values than fine structures with thin fibers and frequent branching points. Pure fibrin clots formed at decreasing NaCl concentrations (135, 100, and 75 mM) presented with increasing mean turbidity values (0.396, 0.628, and 0.757, respectively), and the rate of tPA-mediated plasminogen activation on their surface was inversely related to clot turbidity (Fig. 4B). Composite fibrin/HA clots with turbidity values of 0.502, which is not as high as that of pure fibrin formed at 75 mM NaCl supported plasminogen activation even less than the coarsest pure fibrin. Moreover, relative rates of tPA-mediated plasminogen activation were low on the surface of all types of composite fibrin/HA clots, although the 25 kDa HA-fragment did not increase fibrin thickness or clot turbidity. Thus, we conclude that HA variants of all sizes inhibited tPA-mediated plasminogen activation both in fluid-phase and in fluid-fibrin interface assays.

In our *intrinsic lysis model* 1500 and 500 kDa HA size-variants prolonged clot lysis with plasmin, whereas low molecular-weight HA fragments had no effect (Fig. 5A). If tPA was used to initiate the lysis of fibrin containing plasminogen, the 25 kDa HA fragments also prolonged the lysis time from 31.1±0.7 to 33.6±0.7 min (n=4, p<0.05) in clots with HA/fibrin mass ratio of 0.1 probably related to the abovementioned inhibition of plasminogen activation. The modest 10% increase in tPA-mediated lysis-times could turn into a 1.5-fold change, if the HA/fibrin mass ratio was raised to 2.5 (Fig. 6A). Miniplasmin, lacking the first four kringle domains of plasmin, was a much less efficient fibrinolytic enzyme than plasmin when uniformly dispersed in the clot, but HA additives did not prolong miniplasmin-mediated fibrinolysis (Fig. 5B). We found further differences, if plasmin and miniplasmin were used in our *extrinsic lysis model* (Table 3). Miniplasmin lysed both pure and composite clots significantly faster, and blockage of lysine-binding sites of plasmin with 6-aminohexanoate resulted in clot-lysis acceleration, irrespectively of the presence of native HA. Composite clots containing native HA were more resistant to all fibrinolytic enzymes applied to the clot surfaces: the relative increase in clot lysis time was 1.36-fold for plasmin, and the clot-protective effects of HA was dampened when the lysine-binding sites of plasmin were blocked with 6-aminohexanoate, or miniplasmin was applied. In the course of therapeutic thrombolysis tPA is administered to solubilize preformed clots, which process is mimicked in our other extrinsic fibrinolysis model, when plasminogen is incorporated into clots and tPA is applied on clot surfaces. In the phase of clot formation, the presence of native HA delayed clotting and resulted in a higher maximal clot turbidity in a concentration-dependent way (Fig. 6B), in line with our data on fibrin formation and structure (Table 1, Fig. 1). Composite HA/fibrin clots were less susceptible to tPA-mediated lysis, and increasing the HA/fibrin ratio in the clot resulted in a progressive prolongation of the lysis-time values (Fig. 6B).

This is a preprint version of the paper published in Matrix Biol. 2017 Nov;63:55-68.
doi: 10.1016/j.matbio.2016.12.008.
© 2017 Elsevier. This manuscript version is made available under the CC-BY-NC-ND 4.0 license

3. Discussion

Despite early observations and hypotheses on the presence and role of HA in wound healing, little is known about its modulatory effects on fibrin structure and lytic susceptibility [27]. HA has been described to promote the rate of fibrin formation and increase clot turbidity in a report where typically 0.25-0.75 g/l fibrinogen was clotted with less than 1 nM thrombin, including HA (Mw 32 kDa) up to 4 g/l. It was noted that there was no significant effect up to 0.5 g/l HA [18]. Considering that normal plasma fibrinogen concentrations are 2-4 g/l, these clotting conditions would result in a very loose baseline fibrin structure, as well as an approximate 30-fold molar excess of HA over fibrinogen. Furthermore, at these concentrations, higher molecular weight HA solutions may be technically unmanageable due to their viscosity. These subtle differences from our experimental setup could explain the different results.

Earlier studies on the specific binding of HA to human fibrinogen showed a size-dependence in their interaction, with HA of 36 kDa reaching maximal fibrinogen binding capabilities [17], which is in line with the size-limit we found in the structural-mechanical studies of composite clots (Fig. 1, Table 1). The presence of high-molecular weight HA in the course of clotting resulted in a delayed fibrin formation and a fibrin network with thicker fibers enclosing larger pores. Fibrin fiber thickening in the presence of a modulator could be a result of the intercalation of the modulator in-between protofibrils, as in the case of histones [28]. Our present SAXS data with HA, however, showed an unaltered fibrin protofibril-to-protofibril distance, as well as a preserved longitudinal periodicity reflecting the half-staggered packing of fibrin monomers into fibers. These observations suggest that fiber thickening is most probably due to a higher number of protofibrils with conserved pattern of arrangement in the fibers. The only significant difference in SAXS experiments was found in the broad peak reflecting the typical unit cell size, which has been described earlier as a 19-nm square in the fiber cross-section [25]. Flattening of this peak with the largest HA incorporated at the highest concentration studied (1 g/l) suggests a mild disturbance in the periodic arrangement of the protofibrils across the fiber cross-section. Under conditions, which favour the lateral alignment of fibrin protofibrils, the thickening fibers tend to form fewer branching points, which may explain the higher porosity we found in the HA/fibrin clots. For example, similar clot structures are formed in clots at lower thrombin/fibrinogen ratios, for which viscoelastic parameters have been published previously [29]. Individual fibrin fibers are mechanically more stable, if they are thicker and contain more protofibrils, but the strength of the whole fibrin network is greatly dependent not only on fiber size, but also on branch-point density. Experimental conditions favouring lateral aggregation and stronger fibrin fibers also result in less branching, which weakens network stability; and there are estimated optimal values for fiber thickness (75-90 nm diameter) and branchpoint density (5/μm^3) at which a fibrin clot shows maximal mechanical strength [29]. Our rheology data are in line with the concept that the less frequent branching of thicker (about 100 nm) fibers decreases clot rigidity reflected in lower storage and loss moduli (i.e. less stress is required to gain the same deformation), whereas increased loss tangent (i.e. increased energy loss during deformation) is attributed to an increased intrafiber molecular rearrangement during deformation, which is also facilitated by the lower branch-point density. When increasing shear stress was applied on fibrin/HA clots, the softer clots presented with lower dynamic viscosity values throughout the experiment (i.e. the same stress resulted in higher deformation speed), and gel-fluid transition occurred at lower critical stress values. Although thrombin activity on small synthetic peptide substrate was not influenced by HA, delayed formation of fibrin was observed both in the rheological experiments and some turbidimetric experiments, especially using large HA-variants at high concentrations (Table 1, Figs. 3,6). Large HA molecules at high (1 g/l) concentrations increased the viscosity of the clotting mixture, which may slow down the assembly of protofibrils and besides this kinetic effect, the enhanced binding of large HA to fibrinogen/fibrin monomer [17] may favour the lateral association of protofibrils over frequent branching. Altered fibrin structure properties in the presence of HA might be an advantage, or disadvantage depending on the biological setting, where a composite fibrin/HA matrix is formed. Thicker fibers with larger pores enhance the migration of cancer cells [30], and a softer network may

This is a preprint version of the paper published in Matrix Biol. 2017 Nov;63:55-68.
doi: 10.1016/j.matbio.2016.12.008.
© 2017 Elsevier. This manuscript version is made available under the CC-BY-NC-ND 4.0 license

adapt better to varying space-filling requirements both at wound sites and in tumor environments. At thrombus/plaque interface, however, a less stable clot may favour microembolism [8].

Our study addressed the role of HA-variants on clot lysis in several experimental settings and in all cases we found multiple inhibitory effects. Plasminogen activation by tPA is a key step in the regulation of fibrinolysis, and since the native zymogen adopts a rather compact, activation-resistant conformation, the generation of plasmin by tPA is generally localized to sites of fibrin formation [21,22]. Both tPA and plasminogen bind to fibrin with consequent conformational changes that enable efficient activation on the fibrin surface. Plasminogen activation by tPA was markedly inhibited (70-75 % decrease in activation rate, Table 2) by all HA variants and 6-aminohexanoate, a lysine-analogue blocking kringle domains in plasminogen, did not modify the inhibitory effect of HA. FgDP, a known cofactor for plasminogen activation, however, counteracted the HA-mediated inhibition (Fig. 4A). Measuring plasminogen activation on preformed fibrin surfaces revealed a 4-fold acceleration of plasmin generation, compared to the apparent reaction rate determined in solution without fibrin (Table 2). Plasminogen activation on preformed clots was inhibited by the presence of any HA variant incorporated into fibrin, but the presence of fibrin (similarly to FgDP in Fig. 4A) dampened the extent of inhibition to 30-50 % (Table 2). Thicker fibrin fibers are generally worse cofactors for tPA-mediated plasminogen activation than thinner fibers [22], observations we confirmed in pure fibrin clots of coarser structure prepared at low ionic strength in our experimental setup (Fig. 4B). Low molecular-weight HA fragments, however, do not make the fibrin network any coarser, yet their presence in fibrin resulted in inhibition of plasminogen activation, which suggests that diffusible HA fragments in the fluid-solid boundary layer may mediate similar molecular interactions, as in solution. Apparently, inhibition of tPA-mediated plasminogen activation by HA is not size-dependent, not kringle-dependent, and the availability of FgDP or a fibrin surface can counteract the HA effects.

Once the active protease, plasmin is formed, the next step of fibrinolysis is the proteolytic transsection of fibrin bundles resulting in the disassembly of the clot. Intrinsic lysis models mimic *in vivo* conditions, when fibrinolytic proteases are incorporated into the forming fibrin network. In such situations, plasmin with its 5 kringle domains is an optimally designed fibrinolytic enzyme, once it is bound via kringle$_{1\text{-}3}$ domains to fibrin at the end-to-end junctions between monomers (or is generated by tPA from plasminogen bound to these spots), it can reach with its active site favourable cleavage sites between the E and D domains of fibrin monomers [20,31]. Several studies support the concept that plasmin is a highly processive enzyme, that can crawl on fibrin bundles instead of frequent events of dissociation from and diffusion between fibrin monomers [20,31]. Composite fibrin/HA clots were more resistant to fibrinolysis with incorporated plasmin, when the large HA variants were applied. Large HA variants may act by distorting the proper fibrin structure resulting in a less susceptible substrate, or they may bind to and shield fibrin. Miniplasmin lacking the first 4 kringle domains of plasmin dissolves fibrin much less efficiently, when it is dispersed in the clot, in line with our previous observations, which highlights the importance of fibrin interactions with plasmin kringles 1-4 [32,33]. Lysis-times with incorporated miniplasmin, however, were not prolonged any further by any of the HA variants, which suggests a kringle-dependent mechanism for the plasmin inhibition by HA. This explanation is further supported by our data on the dissolution of HA/fibrin composite clots by surface-applied plasmin or miniplasmin (Table 3), where incorporation of native HA into fibrin retarded plasmin-mediated fibrin dissolution, and removal or blockage of its lysine-binding sites counteracted the HA effect. In such a model, the penetration of surface-applied enzymes into the clot is also an important determinant of the fibrinolytic rate. Typical pore sizes in fibrin do not hinder the diffusion of molecules up to 470 kDa, however, molecules binding to fibrin with high affinity (e.g. tPA) tend to remain bound in a narrow superficial layer [31,32,34]. This phenomenon may explain that faster lysis-times, as observed with miniplasmin in the interfacial lysis assay in contrast with its action in the experimental system with protease uniformly dispersed in the clots, could be reproduced with plasmin after its high-affinity lysine-binding sites were blocked with 6-aminohexanoate both in pure fibrin and in HA/fibrin clots (Table 3).

This is a preprint version of the paper published in Matrix Biol. 2017 Nov;63:55-68.
doi: 10.1016/j.matbio.2016.12.008.
© 2017 Elsevier. This manuscript version is made available under the CC-BY-NC-ND 4.0 license

In summary, our findings characterize HA as a potent modulator of fibrin structure and stability which could have important impact on the role of fibrin in haemostasis, thrombosis, cancer development and wound healing. Throughout our studies HA variants were applied at concentrations in the 0.05-1 g/l range. In our previously published study [8] we found that collagen fragments, decorin and GAGs (chondroitin-sulfate or dermatan-sulfate) exert their maximal modulatory effects at 0.05 g/l concentrations. In our present study, while HA at this low concentration reaches maximal inhibition on tPA-mediated plasminogen activation, and causes significant fibrin fiber thickening as observed by SEM, further increasing the native HA/fibrin ratio progressively boosts fibrin structural changes in preformed clots, as well as fibrinolytic resistance (Fig. 4A, Fig. 6). HA concentrations in the range of 0.01-0.1 mg/l have been reported for normal plasma, and may rise up to 0.2 g/l in rheumatoid arthritis, or liver diseases [11]. There are, however, certain processes, in which fibrin formation occurs at sites where local enrichment in HA has been visualized by histology. At wound sites, high-molecular weight HA quickly accumulates in the first days of the wound healing process, and takes part in forming the provisional fibrin/HA matrix [10]. According to our present data, HA may confer lytic stability of the early fibrin/HA matrix, as well as an improved deformability to shape the wound site. High-molecular weight HA is not only a hygroscopic space-filler, but interacts with lymphocytes and macrophages exerting anti-inflammatory, and anti-angiogenic actions. As the inflammatory phase of wound healing progresses, generation of free radicals and the action of hyaluronidases may degrade high molecular weight HA to smaller, and less fibrin-protective fragments, which also promote inflammation and angiogenesis [10]. Concomitantly, leukocyte activation and neutrophil elastase favour the formation of miniplasmin over plasmin [23,24], the fibrinolytic action of which is less sensitive to HA inhibition, and thus miniplasmin could contribute more efficiently to the removal of the provisional fibrin/HA matrix enabling its replacement with the new tissue. Another extravascular site for fibrin deposition is the solid tumours, which induce capillary leakage and fibrinogen entry into the extracellular matrix, and use it for building a protective fibrin barrier around their cells. Solid tumours are also rich in HA, which has been shown to modify fibrin architecture as to better allow tumour cell migration, and metastasis [30]. Our present data suggest that the anti-fibrinolytic effects of HA may help tumour cells to preserve this protective fibrin shield. In normal human arteries hyaluronic acid is localized to the intima, as well as to the adventitial layer of the vessel wall, which spatially coincides with tissue factor expression, and preferred sites of von Willebrand factor-mediated platelet deposition [35-37]. One could speculate that in adventitia as the most active layer in haemostasis initiation upon vessel wall injury, the locally available high molecular-weight HA might be involved in the temporary stabilization of the primary clot that stops bleeding. Accumulation of hyaluronic acid and versican was also described in restenotic arteries, as well as in the superficial layer of eroded plaques, where it could turn into a thrombus component upon activation of blood coagulation on the plaque surface [12,13]. According to the data of our present study the presence of HA in such locations may also soften the clot mechanically, which could contribute to microembolisation, similarly to decorin and other GAGs as proposed in our earlier work [8].

4. Conclusions

Hyaluronic acid is sparse in circulating plasma, but is enriched in normal vessel wall, as well as in restenotic lesions and eroded plaques of atherosclerotic vessels, i.e. at sites where fibrin is also formed. Composite fibrin/HA matrices may also form at wound sites, and in solid tumours. Native HA and its 500 kDa fragments resulted in thicker fibrin fibers enclosing larger pores and this clot structure was more susceptible to mechanical deformations, but less sensitive to plasmin-catalysed degradation. All HA size-variants inhibited plasminogen activation by tPA through a kringle-independent mechanism. Our data suggest that high-molecular weight HA may favor fibrin network preservation, but could lose its effectiveness upon fragmentation at sites of tissue remodelling and inflammation.

This is a preprint version of the paper published in Matrix Biol. 2017 Nov;63:55-68.
doi: 10.1016/j.matbio.2016.12.008.
© 2017 Elsevier. This manuscript version is made available under the CC-BY-NC-ND 4.0 license

5. Experimental procedures

Human fibrinogen (plasminogen free) was the product of Calbiochem (LaJolla, California, USA). The chromogenic substrates for plasmin Spectrozyme-PL (H-D-norleucyl-hexahydrotyrosyl-lysine-p-nitroanilide), for tPA Spectrozyme-tPA (methylsulfonyl-D-cyclohexylalanyl-glycyl-arginine-p-nitroanilide) and for thrombin Spectrozyme-TH (H-D-hexahydrotyrosyl-L-alanyl-L-arginine-p-nitroanilide), as well as cyanogenbromide human fibrinogen fragments (FgDP) were from Sekisui Diagnostics (Pfungstadt, Germany), and the tPA was from Boehringer Ingelheim (Germany). Bovine thrombin purchased from Serva (Heidelberg, Germany) was further purified by ion-exchange chromatography on sulfopropyl-Sephadex yielding preparation with specific activity of 2,100 IU/mg [38] and 1 IU/ml was considered equivalent to approximately 10.7 nM by active site titration [39]. Miniplasmin was prepared as previously described [33].

5.1. Generation of HA size-variants

High molecular weight HA of 1,500 kDa was provided by the Matrix Biology Institute (Edgewater, NJ, USA). This native HA was further processed by sonication or acidic treatment to generate lower molecular weight fragments as previously published [40,41]. Briefly, 500 kDa HA was generated by sonication of 5 g/l native HA in distilled water on the ice with a Branson Sonifier 250 (Branson Ultrasonics Corp., Danbury,CT) applying 4 times 30 second-long pulses with intermittent 1 min pauses at 50% duty cycle and the maximal output setting for micro tips. Low molecular weight HA fragments of 25 kDa were prepared by acidic hydrolysis: 10 g/l native HA was incubated in 0.1 M HCl for 24 hours at 60 °C followed by neutralization with equimolar NaOH. Molecular weights of the HA variants were verified by comparison against commercial HA preparations of known sizes (three polydisperse HA preparations with molecular weights of 15-30 kDa, 120-350 kDa and 1000-1250 kDa, from Sigma-Aldrich Kft., Budapest, Hungary) using agarose gel electrophoresis and visualization of the GAGs with the dye Stains-All (3,3'-dimethyl-9-methyl-4,5,4',5'-dibenzothiacarbocyanine, from Sigma-Aldrich) [42].

5.2. Characterization of the composite fibrin/HA clot structure

5.2.1. Scanning electron microscopy (SEM) was used for the quantitative description of fiber thickness in the fibrin network structures. Fibrin clots were prepared in duplicate: 6 μM fibrinogen in 10 mM HEPES buffer pH 7.4 containing 150 mM NaCl (HBS) was clotted with 5 nM thrombin at 37°C for 1 h, with or without 0.05 or 0.2 g/l HA of various sizes. Clots were processed, as detailed previously [8] and images were taken with scanning electron microscope EVO40 (Carl Zeiss GmbH, Oberkochen, Germany). SEM images were analyzed to determine the diameter of the fibrin fibers using self-designed program functions running under the Image Processing Toolbox v. 9.4 of Matlab R2016a (The Mathworks, Natick, MA) as previously described [22,43].

5.2.2. Fluid permeability of clots was measured to assess the porosity of the fibrin network [44]. Fibrin clots were formed at the bottom of disposable plastic pipette tips using 15 nM thrombin and 7.4 μM fibrinogen in HBS, and the HA size-variants at 0, 0.25, or 0.5 g/l. After 70 min of clotting at 37°C, fluid passing through the clots was measured in a collecting tube attached to the bottom of the clot, while hydrostatic pressure between the top surface of the buffer reservoir and the clot bottom was kept constant. The permeability coefficient, K_s was calculated, as previously published [44].

5.2.3. Viscoelastic properties of the fibrin/HA clots were studied with oscillation rheometry [8]. Fibrinogen (7.4 μM in HBS) was pre-mixed with 0.05, 0.2 or 1 g/l HA variants, and after the addition of 10 nM thrombin the clotting mixture was immediately transferred to the stationary plate of HAAKE RheoStress 1 oscillation rheometer (Thermo Scientific, Karlsruhe, Germany). The cone (Titanium, 2° angle, 35 mm diameter) of the rheometer was brought to the gap position and an oscillatory shear strain (γ) of 0.015 at 1 Hz was imposed at 2 min after the addition of thrombin. Measurements of storage modulus (*G'*) and loss modulus (*G''*) were taken for 10 min with HAAKE RheoWin data manager software v. 3.50.0012 (Thermo Scientific). Following this 10-min clotting phase determination of the flow limit of the fibrin gels was performed in the same samples

This is a preprint version of the paper published in Matrix Biol. 2017 Nov;63:55-68.
doi: 10.1016/j.matbio.2016.12.008.
© 2017 Elsevier. This manuscript version is made available under the CC-BY-NC-ND 4.0 license

increasing stepwise the applied shear stress (τ) from 0.01 to 400.0 Pa in the course of 120 s and the resulting measured strain was used for calculation of the viscosity modulus (the critical shear stress τ_0 determined by extrapolation of the fall in viscosity to 0 was used as indicator of the gel/fluid transition in the fibrin structure).

5.2.4. Structural characterization of fibrin by small-angle X-ray scattering (SAXS). Fibrinogen (7.4 μM in HBS) containing 0, 0.2 or 1 g/l HA size-variants was clotted with 5 nM thrombin, and the generated fibrin structures were examined by SAXS measurements performed on the four-crystal monochromator beamline of Physikalisch-Technische Bundesanstalt (PTB, Berlin, Germany) supplemented by the SAXS setup of Helmholtz-Zentrum Berlin at the synchrotron radiation facility BESSY II (HZB, Berlin, Germany) [28,45].

5.3. Plasminogen activation assays

Plasminogen activation by tPA in solution was followed in 96-well microtiter plates. A mixture of 3 nM tPA and 0.6 mM Spectrozyme-PL in HBS was added to plasminogen at 200 nM final concentration and other additives: 0.1 g/l FgDP, 0.5 mM 6-aminohexanoate and HA size-variants in the range of 0.05-0.5 g/l final concentration. The generated plasmin released p-nitroaniline from Spectrozyme-PL, the absorbance of which was continuously recorded at 405 nm (A_{405}) with Zenith 200rt spectrophotometer (Anthos Labtec Instruments GmbH, Salzburg, Austria). The measured values were plotted versus time squared (t^2) yielding a linear relationship according to the equation $\Delta A_{405}=0.5\varepsilon k_1 k_{cat}[tPA]\ t^2$ [8], where ε=1.76 mM^{-1} is the extinction coefficient of p-nitroaniline, k_1=810 min^{-1} is the turn-over number of plasmin on Spectrozyme-PL, k_{cat} and $[tPA]$ are the catalytic constant in plasminogen activation and the concentration of tPA in the mixture, respectively. The term $V_{app}=k_{cat}[tPA]$ is equivalent to the apparent maximal rate of plasminogen activation and was determined from linear regression according to the abovementioned equation (Curve fitting toolbox v. 3.5.3 of Matlab 2016a).

For evaluating composite fibrin/HA matrices, as surfaces to support plasminogen activation, 6 μM fibrinogen containing 200 nM plasminogen, and up to 0.5 g/l HA size-variants in HBS was clotted by 100 nM thrombin. After 45 min clotting the activation of plasminogen in the clot was initiated by layering 3 nM tPA and 0.6 mM Spectrozyme-PL in HBS on the clot surfaces. For comparison, some pure fibrin clots were formed at lower NaCl concentrations (75 mM, 100 mM, or 135 mM NaCl) known to result in a coarser fibrin network. The formation of plasmin in the clot-fluid phase boundary layer was followed and evaluated, as described above [46].

5.4. Turbidimetric fibrinolytic assays

Formation and dissolution of fibrin/HA clots were followed in 96-well microtiter plates by measuring the light absorbance at 340 nm at 37°C with a Zenyth 200rt microplate spectrophotometer (HA solutions up to 2 g/l concentration did not show any turbidity signal).

Intrinsic fibrinolysis was initiated by mixing (i) tPA and plasminogen or (ii) plasmin or miniplasmin in the clot at the time of the initiation of clotting by thrombin. In these experimental setups fibrin formation and dissolution are concurring processes. For tPA-induced fibrinolysis (i) 6 μM fibrinogen in HBS containing 30 nM plasminogen and 0.2 g/l HA variants was clotted with 20 nM thrombin in the microplate well, and 1 nM tPA was also included in the clotting mixture. In model (ii) 6 μM fibrinogen in HBS containing 0.2 g/l HA variants was mixed with 20 nM thrombin, and 6 nM plasmin (or miniplasmin) in the well. In certain experiments the significance of the fibrin/HA ratio was evaluated in clots containing 1.2 μM fibrinogen and 2 g/l native HA.

In our two *extrinsic fibrinolysis* models dissolution of preformed clots was initiated by applying enzymes on the clot surface. For tPA-induced fibrinolysis (i) 6 μM fibrinogen in HBS containing 220 nM plasminogen and 0, 0.2 or 1 g/l native HA was clotted with 100 nM thrombin in the wells and fibrin formation was followed by turbidimetry. After 50 min of clotting, fibrinolysis was initiated by layering 14 nM tPA on the surface of the clots and the turbidimetric measurement was continued to detect the dissolution process. As an alternative (ii), plasminogen was omitted from the

This is a preprint version of the paper published in Matrix Biol. 2017 Nov;63:55-68.
doi: 10.1016/j.matbio.2016.12.008.
© 2017 Elsevier. This manuscript version is made available under the CC-BY-NC-ND 4.0 license

fibrinogen/HA mixture, and lysis of the preformed clot was initiated by surface-applied 500 nM (mini)plasmin. The role of the lysine-binding sites located on the kringle domains missing in miniplasmin was studied by including the blocking lysine-analogue 6-aminohexanoate at 0.5 mM concentration in the (mini)plasmin solution.

For quantitation of the turbidimetric experiments clotting time was defined as the time needed to reach 90 % of maximal clot turbidity, whereas lysis time (t_{50}) was defined as the time after the addition of the lytic enzyme needed to reduce the turbidity of the clot to a half-maximal value in the course of its dissolution.

5.5. Statistical analysis

The distribution of the data on fiber diameter was analysed according to an algorithm used previously [22,43]: theoretical distributions were fitted to the empirical data sets and compared using Kuiper test and Monte Carlo simulation procedures. The statistical evaluation of other experimental measurements in this report was performed with Kolmogorov-Smirnov test (Statistics Toolbox 10.2 of Matlab R2016a).

Author contributions

EK and KK conceived and coordinated the study, designed the experiments and wrote the paper; EK and NB performed the rheometry, permeability and lytic measurements and analysed the data; ZV and AB performed the SAXS measurements and analysed the data; LS performed the electron microscopic measurements and analysed the data.

Acknowledgements

The authors are grateful to Györgyi Oravecz and Krisztián Bálint for technical assistance. This work was supported by the Hungarian Scientific Research Fund OTKA 112612.

Conflict of interest

None to declare.

This is a preprint version of the paper published in Matrix Biol. 2017 Nov;63:55-68.
doi: 10.1016/j.matbio.2016.12.008.
© 2017 Elsevier. This manuscript version is made available under the CC-BY-NC-ND 4.0 license

References

[1] M.W. Mossesson, Fibrinogen and fibrin structure and functions, J. Thromb. Haemost. 3 (2005) 1894-1904.

[2] N. Laurens, P. Koolwijk, M.P.M. De Maat, Fibrin structure and wound healing, J. Thromb. Haemost. 4 (2006) 932-939.

[3] M.E. Carr Jr, D.A. Gabriel, J. McDonagh, Influence of Ca2+ on the structure of reptilase-derived and thrombin-derived fibrin gels, Biochem. J. 239 (1986) 513-516.

[4] B. Blomback, K. Carlsson, B. Hessel B, Native fibrin gel networks observed by 3D microscopy, permeation and turbidity, Biochim. Biophys. Acta 997 (1989) 96-110.

[5] J.W. Weisel, R.I. Litvinov, Mechanisms of fibrin polymerization and clinical implications, Blood 121 (2013) 1712-1719.

[6] A. Undas, R.A.S. Ariens, Fibrin clot structure and function. A role in the pathophysiology of arterial and venous thromboembolic diseases, Arterioscler. Thromb. Vasc. Biol. 31 (2011) e88-e99.

[7] R.S. Schwartz, A. Burke, A. Farb, D. Kaye , J.R. Lesser, T.D. Henry , R. Virmani, Microemboli and microvascular obstruction in acute coronary thrombosis and sudden coronary death: relation to epicardial plaque histopathology, J. Am. Coll. Cardiol. 54 (2009) 2167-2173.

[8] Z. Rottenberger, E. Komorowicz, L. Szabo, A. Bota, Z. Varga, R. Machovich, C. Longstaff, K. Kolev, Lytic and mechanical stability of clots composed of fibrin and blood vessel wall components, J. Thromb. Haemost. 11 (2013) 529-538.

[9] B.P.Toole, T.N.Wight, M.L. Tammi, Hyaluronan-cell interactions in cancer and vascular disease, J. Biol. Chem. 277(2002) 4593-4596.

[10] K.L. Aya, R. Stern, Hyaluronan in wound healing: Rediscovering a major player, Wound Rep. Reg. 22 (2014) 579-593.

[11] M.K. Cowman, H.G. Lee, K.L. Schwertfeger, J.B. McCarthy, E.A. Turley, The content and size of hyaluronan in biological fluids and tissues, Front. Immunol. 6 (2015) 261.

[12] F.D. Kolodgie, A.P. Burke, T.N. Wight, R. Virmani, The accumulation of specific types of proteoglycans in eroded plaques: a role in coronary thrombosis in the absence of rupture, Curr. Opin. Lipidol. 15 (2004) 575-582.

[13] T.N. Wight, M.J. Merrilees, Proteoglycans in atherosclerosis and restenosis. Key roles for versican, Circ. Res. 94 (2004) 1158-1167.

[14] S. Reitsma, D.W. Slaaf, H. Vink H, M.A. van Zandvoort, M.G. oude Egbrink, The endothelial glycocalix: composition, functions, and visualization, Pflugers Arch. – Eur. J. Physiol. 454 (2007) 345-359.

[15] N. Nagy, T. Freudenberger, A. Melchior-Becker, K. Röck, M. Ter Braak, H. Jastrow, M. Kinzig, S. Lucke, T. Suvorava, G. Kojda, A.A. Weber, F. Sörgel, B. Levkau, S. Ergün, J.W. Fischer, Inhibition of

This is a preprint version of the paper published in Matrix Biol. 2017 Nov;63:55-68.
doi: 10.1016/j.matbio.2016.12.008.
© 2017 Elsevier. This manuscript version is made available under the CC-BY-NC-ND 4.0 license

hyaluronan synthesis accelerates murine atherosclerosis. Novel insights into the role of hyaluronan synthesis, Circulation, 122 (2010) 2313-2322.

[16] J.M. Cyphert, C.S. Trempus, S. Garantziotis, Size matters: molecular weight specificity of hyaluronan effects in cell biology, Int. J. Cell. Biol. 2015 (2015) 67-74.

[17] R.D. LeBeuf, R.H. Raja, G.M. Fuller, P.H. Weigel, Human fibrinogen specifically binds hyaluronic acid, J. Biol. Chem. 261 (1986) 12586-12592.

[18] R.D. LeBeuf, R.R. Gregg, P.H. Weigel, G.M. Fuller, Effects of hyaluronic acid and other glucosaminoglycans on fibrin polymer formation, Biochemistry 26 (1987) 6052-6057.

[19] C. Longstaff, K. Kolev, Basic mechanisms and regulation of fibrinolysis, J. Thromb. Haemost. 13(Suppl 1) (2015) S98-S105.

[20] J.W. Weisel, R.I. Litvinov, The biochemical and physical process of fibrinolysis and effects of clot structure and stability on the lysis rate, Cardiovasc. Hematol. Agents. Med. Chem. 6 (2008) 161-180.

[21] M. Hoylaerts, D.C. Rijken, H.R. Lijnen, D. Collen, Kinetics of the activation of plasminogen by human tissue plasminogen activator. Role of fibrin, J. Biol. Chem. 257 (1982) 2912-2919.

[22] C. Longstaff, C. Thelwell, S.C. Williams, M.M. Silva, L. Szabó, K. Kolev, The interplay between tissue plasminogen activator domains and fibrin structures in the regulation of fibrinolysis: kinetic and microscopic studies, Blood 117 (2011) 661-668.

[23] L.A. Moroz, Mini-plasminogen: a mechanism for leukocyte modulation of plasminogen activation by urokinase, Blood 58 (1981) 97-104.

[24] R. Machovich, W.G. Owen, An elastase-dependent pathway of plasminogen activation, Biochemistry, 28 (1989) 4517-4522.

[25] C. Yeromonahos, B. Polack, F. Caton, Nanostructure of the fibrin clot, Biophys. J. 99 (2010) 2018-2027.

[26] J.W. Weisel, The electron microscope band pattern of human fibrin: various stains, lateral order, and carbohydrate localization, J. Ultrastruct. Mol. Struct. Res. 96 (1986) 176-188.

[27] P.H. Weigel, G.M. Fuller, R.D. LeBeuf, A model for the role of hyaluronic acid and fibrin in the early events during the inflammatory response and wound healing, J. Theor. Biol. 119 (1986) 219-234.

[28] C. Longstaff, I. Varju, P. Sotonyi, L. Szabó, M. Krumrey, A. Hoell, A. Bóta, Z. Varga, E. Komorowicz, K. Kolev, Mechanical stability and fibrinolytic resistance of clots containing fibrin, DNA, and histones, J. Biol. Chem. 288 (2013) 6946-6956.

[29] E.A. Ryan, L.F. Mockros, J.W. Weisel, L. Lorand, Structural origins of fibrin clot rheology, Biophys. J. 77 (1999) 2813-2826.

[30] W. Hayen, M. Goebeler, S. Kumar, R. Riessen, V. Nehls, Hyaluronan stimulates tumor cell migration by modulating the fibrin fiber architecture, J Cell Sci (1999) 2241-2251.

This is a preprint version of the paper published in Matrix Biol. 2017 Nov;63:55-68.
doi: 10.1016/j.matbio.2016.12.008.
© 2017 Elsevier. This manuscript version is made available under the CC-BY-NC-ND 4.0 license

[31] K. Kolev, C. Longstaff, R. Machovich, Fibrinolysis at the fluid-solid interface of thrombi, Curr. Med. Chem.- Cardiovasc. Hematol. Agents 3 (2005) 341-355.

[32] K. Kolev, K. Tenekedjiev, E. Komorowicz E, R. Machovich, Functional evaluation of the structural features of proteases and their substrate in fibrin surface degradation, J. Biol. Chem. 272 (1997) 13666-13675.

[33] E. Komorowicz, K. Kolev, R. Machovich, Fibrinolysis with des-kringle derivatives of plasmin and its modulation by plasma protease inhibitors, Biochemistry 37 (1998) 9112-9118.

[34] J.P. Collet, D. Park, C. Lesty, J. Soria, C. Soria, G. Montalescot, J.W. Weisel, Influence of fibrin network conformation and fibrin fiber diameter on fibrinolysis speed. Dynamic and structural approaches by confocal microscopy, Arterioscler. Thromb. Vasc. Biol. 20 (2000) 1354-1361.

[35] R. Riessen, T.N. Wight, C. Pastore, C. Henley, J.M. Isner, Distribution of hyaluronan during extracellular matrix remodeling in human restenotic arteries and balloon-injured rat carotid arteries, Circulation 93 (1996) 1141-1147.

[36] J.N. Wilcox, K.M. Smith, S.M. Schwartz, D. Gordon, Localization of tissue factor in the normal vessel wall and in the atherosclerotic plaque, Proc. Natl. Acad. Sci. USA 86 (1989) 2839-2843.

[37] E. Komorowicz, R.D. McBane, J. Charlesworth, D.N. Fass, Reduced high shear platelet adhesion to the vascular media: Defective von Willebrand factor binding to the interstitial collagen, Thromb. Haemost. 87 (2002) 763-770.

[38] R.L. Lundblad, H.S. Kingdon, K.G. Mann, Thombin, Methods Enzymol. 45 (1976) 156-176.

[39] C. Longstaff, M.Y. Wong, P.J. Gaffney, An international collaborative study to investigate standardisation of hirudin potency, Thromb. Haemost. 69 (1993) 430-435.

[40] C.M. McKee, M.B. Penno, M. Cowman, M.D. Burdick, R.M. Strieter, C. Bao, P.W. Noble, Hyaluronan (HA) fragments induce chemokine gene expression in alveolar macrophages. The role of HA size and CD44, J. Clin. Invest. 98 (1996) 2403-2413.

[41] K. Tommeraas, C. Melander, Kinetics of hyaluronan hydrolysis in acidic solution at various pH values, Biomacromolecules 9 (2008) 1535-1540.

[42] M.K. Cowman, C.C. Chen, M. Pandya, H. Yuan, D. Ramkishun, J. LoBello, S. Bhilocha, S. Russell-Puleri, E. Skendaj, J. Mijovic, W. Jing, Improved agarose gel electrophoresis method and molecular mass calculation for high molecular mass hyaluronan, Anal. Biochem. 417 (2011) 50-56.

[43] N.D. Nikolova, D. Toneva-Zheynova, K. Kolev, K. Tenekedjiev, Monte Carlo statistical tests for identity of theoretical and empirical distributions of experimental data, in: W.K. Chan (Ed.), Theory and Applications of Monte Carlo Simulations, InTech, 2013, pp. 1-26.

[44] I. Varju, C. Longstaff, L. Szabo, A.Z. Farkas, V.J. Varga-Szabó, A. Tanka-Salamon, R. Machovich, K. Kolev, DNA, histones and neutrophil extracellular traps exert anti-fibrinolytic effects in a plasma environment, Thromb. Haemost. 113 (2015) 1289-1298.

This is a preprint version of the paper published in Matrix Biol. 2017 Nov;63:55-68.
doi: 10.1016/j.matbio.2016.12.008.
© 2017 Elsevier. This manuscript version is made available under the CC-BY-NC-ND 4.0 license

[45] G. Gleber, S. Cibik, S. Haas, A. Hoell, P. Müller, M. Krumrey, Traceable size determination of PMMA nanoparticles based on Small Angle X-ray Scattering (SAXS), J. Phys. Conf. Ser. 247 (2010) 012027.

[46] C. Longstaff, C.M. Whitton, A proposed reference method for plasminogen activators that enables calculation of enzyme activities in SI units, J. Thromb. Haemost. 2 (2004) 1416-1421.

This is a preprint version of the paper published in Matrix Biol. 2017 Nov;63:55-68.
doi: 10.1016/j.matbio.2016.12.008.
© 2017 Elsevier. This manuscript version is made available under the CC-BY-NC-ND 4.0 license

Figure Legends

Figure 1. Scanning electron microscopic images of composite fibrin/hyaluronic acid clots. SEM images of pure fibrin (A), and composite fibrin clots containing 0.2 g/L native HA (B) or HA fragments of 500 kDa (C) and 25 kDa (D). Scale bar=1 μM (applies for all images).

Figure 2. Small angle X-ray scattering pattern of fibrin. Pure fibrin and composite HA/fibrin clots containing 0.2 or 1 g/l of the indicated HA size-variants were prepared as described in Experimental procedures. SAXS curves are shifted vertically by the factors indicated at their origin for better visualization. The *dashed vertical line* indicates the longitudinal periodicity of about 22 nm in fibrin fibers, the *broad peak between 4 and 10 nm* reflects the lateral packing of protofibrils, and *the broad peak between 12.5 and 31 nm* describes the cluster unit cell periodicity in the fibers.

Figure 3. Modification of the viscoelastic properties of fibrin by native hyaluronic acid. ***A***: Fibrinogen (7.4 μM) containing 0 (black) or 0.2 g/l native HA (red) was mixed with thrombin and storage modulus (G', continuous line) and loss modulus (G'', dashed line) were measured in an oscillation rheometer. ***B***: Following 10-min clotting, stepwise increasing shear stress τ was applied to fibrin formed in the gap space of the rheometer and viscosity (η) was measured. Representative curves with two parallels are shown. G', G'' values and their ratios (loss tangents) at the end of the 10-min clotting, as well as the critical values τ_0, which define the gel/fluid transition of fibrin/HA clots are summarized in Table 1.

Figure 4. Plasminogen activation by tPA. ***A: In solution***. Plasminogen activation by tPA in the absence (black) or presence of additives: 100 mg/l FgDP (blue), 50 mg/l native HA (purple), or both in combination (green)) was followed by continuous measurement of p-nitroaniline release from the plasmin substrate Spectrozyme-PL. Absorbance at 405 nm cumulates as a quadratic function of time t, according to the equation of $\Delta A_{405}=0.5\varepsilon k_1 V_{app} t^2$ as detailed in Experimental procedures. ***Inset***: ***Effects of 6-aminohexanoate and FgDP on the inhibition of plasminogen activation by HA***. Rates of plasminogen activation in the absence (black triangles) or presence (blue triangles) of 100 mg/l FgDP or in the presence of 0.5 mM 6-aminohexanoate (red circles) in solution containing native HA at increasing concentrations are presented relative to the activation rate in the HA-free solution. Mean and standard deviation for n=5-10 experiments are shown. ***B: Plasminogen activation on the surface of fibrin***. Fibrin clots containing plasminogen and native HA were prepared and following addition of 3 nM tPA and the plasmin substrate Spectrozyme-PL the absorbance was continuously measured at 405 nm (A_{405}). Secondary, linearized plots of the raw data, as in panel A, are presented for pure fibrin polymerized in the presence of 135 mM (black), 100 mM (blue), and 75 mM NaCl (green), and for fibrin containing 0.5 g/l native HA, polymerized in 135 mM NaCl (red). Curves represent mean values for n=5-10 experiments.

Figure 5. Intrinsic fibrinolysis mediated by (mini)plasmin incorporated in fibrin clots containing hyaluronic acid size-variants. Clots were prepared from 6 μM fibrinogen containing none (black), or 0.2 g/l HA of 1500 kDa (blue), 500 kDa (green) or 25 kDa (red) average molecular mass. Fibrinolytic enzymes (6 nM) were added at the same time as thrombin (20 nM) resulting in their homogenous distribution inside the clots. Formation and lysis of clots was monitored by continuous recording of the absorbance at 340 nm (A_{340}). Representative experiments are shown for plasmin (panel **A**) or miniplasmin (panel **B**).

Figure 6. tPA-mediated fibrinolysis in clots at various hyaluronic acid/fibrin ratios. ***A:*** Clots were prepared from 1.2 μM fibrinogen, containing 28 nM plasminogen and none (black), 0.1 g/l (red) or 1 g/l (blue) native HA. tPA (0.6 nM) was added at the same time as thrombin (20 nM) resulting in simultaneous clotting and tPA-mediated fibrinolysis. ***B:*** Composite HA/fibrin clots containing 6 μM

This is a preprint version of the paper published in Matrix Biol. 2017 Nov;63:55-68.
doi: 10.1016/j.matbio.2016.12.008.
© 2017 Elsevier. This manuscript version is made available under the CC-BY-NC-ND 4.0 license

fibrin, 220 nM plasminogen, and 0 (black), 0.2 (red) or 1 g/l (blue) native HA were prepared and fibrinolysis was initiated by the addition of 14 nM tPA on top of the preformed clots (indicated by the arrow in the graph). Formation and dissolution of the fibrin network was followed at 340 nm in a microplate reader (A_{340}), curves represent mean values+/- standard deviation, n=4.

This is a preprint version of the paper published in Matrix Biol. 2017 Nov;63:55-68.
doi: 10.1016/j.matbio.2016.12.008.
© 2017 Elsevier. This manuscript version is made available under the CC-BY-NC-ND 4.0 license

Table 1. Structural characteristics of composite fibrin/hyaluronic acid clots.

		Additive			
		none	HA 1500 kDa	HA 500 kDa	HA 25 kDa
clotting time (min)		25.4±3.7	31.9*±3.3	30.9*±4.5	25.4±2.6
maximal clot turbidity		0.300±0.018	0.372*±0.009	0.362*±0.019	0.301±0.010
fibrin fiber diameter (nm)		86.3 (70.5-104.3)	97.2* (78.0-119.4)	98.6* (80.6-120.5)	80.4* (65.8-98.1)
fluid permeability coefficient (K_s, 10^{-9} cm^2)		0.71±0.05	1.14*±0.09	1.07*±0.11	0.86*±0.03
viscoelastic parameters	G' (Pa)	34.05±8.31	22.21*±5.5	18.23*±4.33	24.19±6.40
	G'' (Pa)	3.10±0.51	2.28*±0.52	1.98*±0.39	2.48±0.50
	G''/G' (-)	0.092±0.009	0.104*±0.009	0.110*±0.011	0.104±0.011
	τ_0 (RU)	1.00±0.13	0.65*±0.12	0.79*±0.15	0.81±0.15

Fibrin clots containing various HA size-variants at 0.2 g/L were prepared from 2.5 g/l fibrinogen for turbidimetry, scanning electronmicroscopy, fluid permeability and oscillation rheometry experiments to evaluate key structural and physical determinants of the composite fibrin networks (maximal clot turbidity and clotting time, fibrin fiber diameter, fluid permeability coefficient reflecting porosity and viscoelastic parameters reflecting mechanical strength as described in Experimental procedures). Plateau values of storage modulus (*G'*), loss modulus (*G''*) and loss tangent (G''/G') at complete clotting (Fig. 3A) are presented. The critical shear stress for the gel/fluid transition in the fibrin structure (τ_0) illustrated in Fig. 3B is expressed in relative units (RU) compared to pure fibrin. Asterisks indicate $p<0.05$ according to Kolmogorov-Smirnov test in comparison to pure fibrin, n=4-12, values are reported as mean±standard deviation or median and bottom-top quartile range in parenthesis.

This is a preprint version of the paper published in Matrix Biol. 2017 Nov;63:55-68.
doi: 10.1016/j.matbio.2016.12.008.
© 2017 Elsevier. This manuscript version is made available under the CC-BY-NC-ND 4.0 license

Table 2. Plasminogen activation in the presence of hyaluronic acid size-variants.

Additive	none	HA 1500 kDa	HA 500 kDa	HA 25 kDa
V_{app} in solution (nM/min)	0.192 (0.017)	0.071 (0.012)*	0.050 (0.005)*	0.050 (0.011)*
V_{app} on the surface of the clot (nM/min)	0.776 (0.154)	0.499 (0.109)*	0.579 (0.106)*	0.360 (0.045)*

Plasminogen activation by tPA in the absence or presence of HA size-variants at 0.5 g/l in solution or on the surface of pre-formed fibrin clots containing plasminogen was followed by continuous measurement of the cleavage of Spectrozyme-PL and activation rates were determined from the slopes of linearized plots illustrated in Fig. 4. Mean and standard deviation in parenthesis of n=5-10 measurements are shown, asterisk indicates $p<0.05$ according to Kolmogorov-Smirnov test in comparison to no additive.

This is a preprint version of the paper published in Matrix Biol. 2017 Nov;63:55-68.
doi: 10.1016/j.matbio.2016.12.008.
© 2017 Elsevier. This manuscript version is made available under the CC-BY-NC-ND 4.0 license

Table 3. Dissolution of preformed composite fibrin/hyaluronic acid clots by plasmin or miniplasmin applied to their surface.

	Lysis time (min)		Relative effect
Additive in fibrin	none	HA 1500 kDa	HA 1500 kDa
Plasmin	49.29 (5.03)	67.00 (8.14) *¶	1.36
Plasmin + 6AH	42.48 (7.57) *£	53.85 (4.54) ¶£	1.26
Miniplasmin	42.09 (4.37) *	48.67 (5.67) ¶	1.16

Clots containing 6 μM fibrin with or without 0.5 g/l of native HA were prepared and fibrinolysis was initiated with 500 nM plasmin or miniplasmin applied with or without 0.5 mM 6-aminohexanoate (6AH) on the clot surface. Lysis times were defined as the time (min) needed to reach half-maximal turbidity on the descending part of the turbidity curves and their values are reported as mean with standard deviation in parenthesis, n=4-8. Symbols indicate $p<0.05$ according to Kolmogorov-Smirnov test in comparison to 1) 6AH-free plasmin-mediated lysis of pure fibrin (*), 2) 6AH-free plasmin on identical clot-type (£), 3) additive-free clot with identical enzyme (¶).

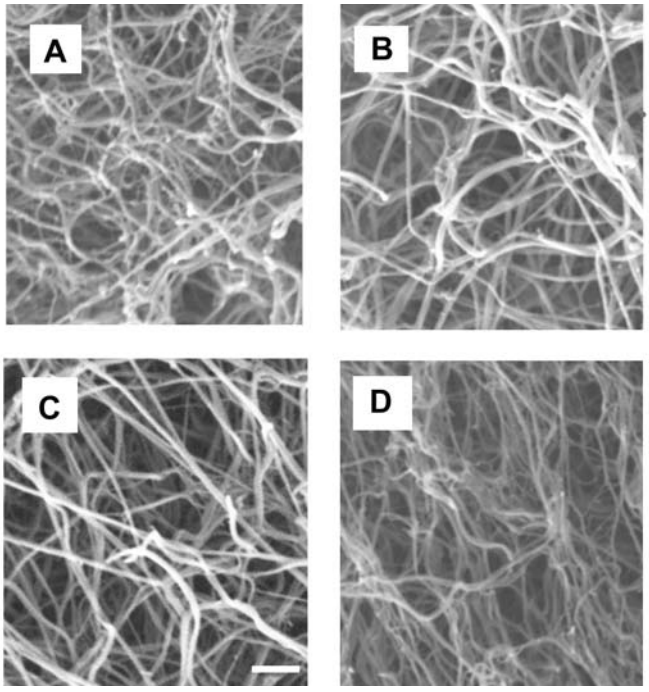

Figure 1

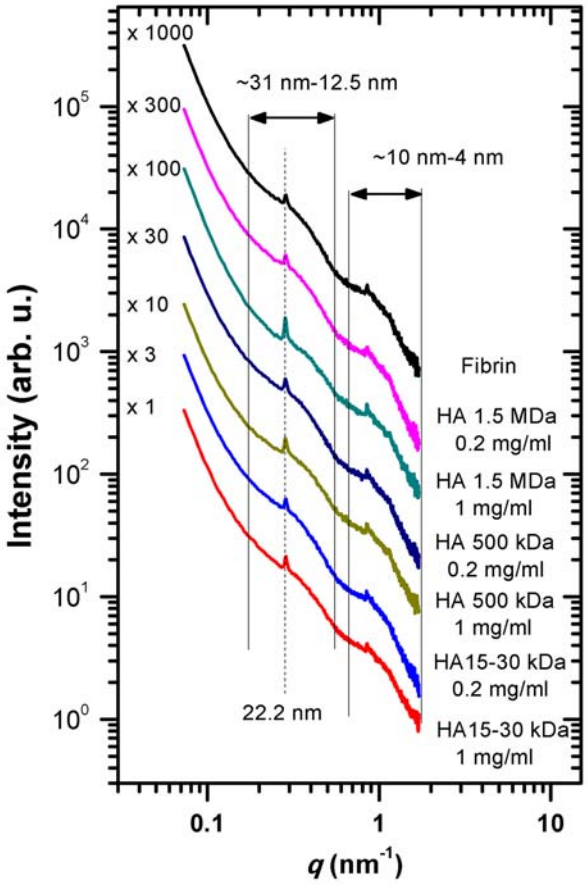
x 1000
x 300
x 100
x 30
x 10
x 3
x 1
~31 nm-12.5 nm
~10 nm-4 nm
22.2 nm
Fibrin
HA 1.5 MDa
0.2 mg/ml
HA 1.5 MDa
1 mg/ml
HA 500 kDa
0.2 mg/ml
HA 500 kDa
1 mg/ml
HA15-30 kDa
0.2 mg/ml
HA15-30 kDa
1 mg/ml
Intensity (arb. u.)
10^0
10^1
10^2
10^3
10^4
10^5
0.1
1
10
q (nm^{-1})

Figure 2

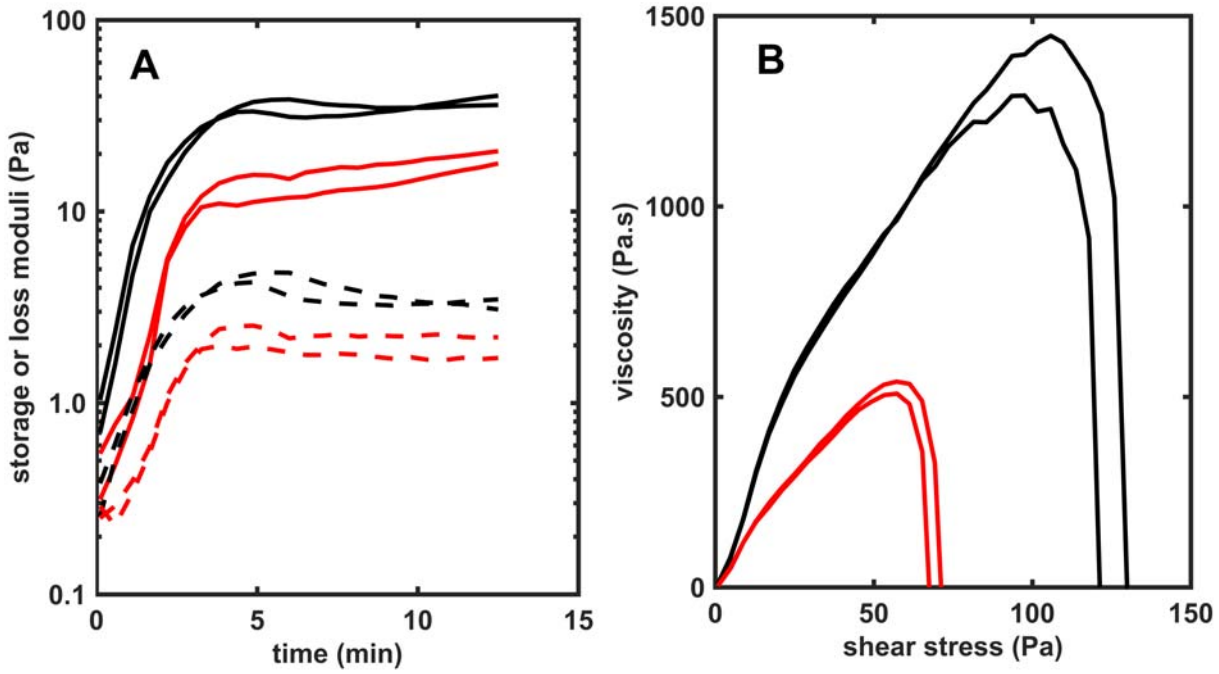
A
B
storage or loss moduli (Pa)
time (min)
viscosity (Pa.s)
shear stress (Pa)
100
10
1.0
0.1
0
5
10
15
1500
1000
500
0
50
100
150

Figure 3

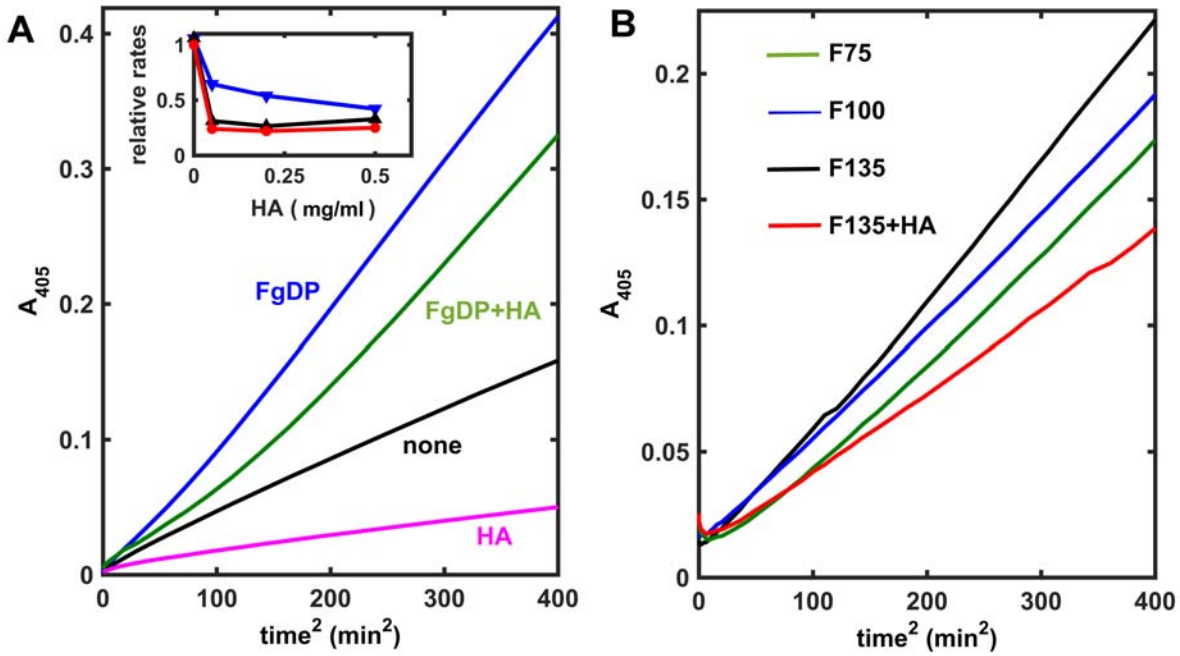
A
B
relative rates
HA (mg/ml)
FgDP
FgDP+HA
none
HA
F75
F100
F135
F135+HA
A405
time2 (min2)

Figure 4

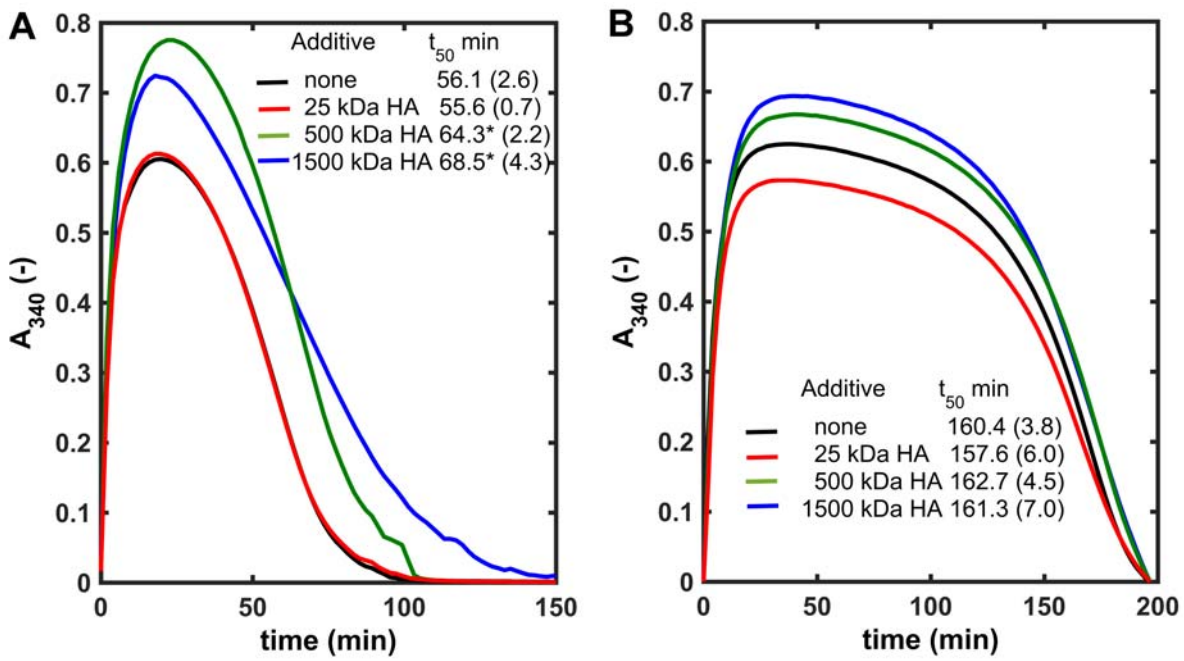
A
B
Additive
t_{50} min
none 56.1 (2.6)
25 kDa HA 55.6 (0.7)
500 kDa HA 64.3* (2.2)
1500 kDa HA 68.5* (4.3)
none 160.4 (3.8)
25 kDa HA 157.6 (6.0)
500 kDa HA 162.7 (4.5)
1500 kDa HA 161.3 (7.0)
A_{340} (-)
time (min)

Figure 5

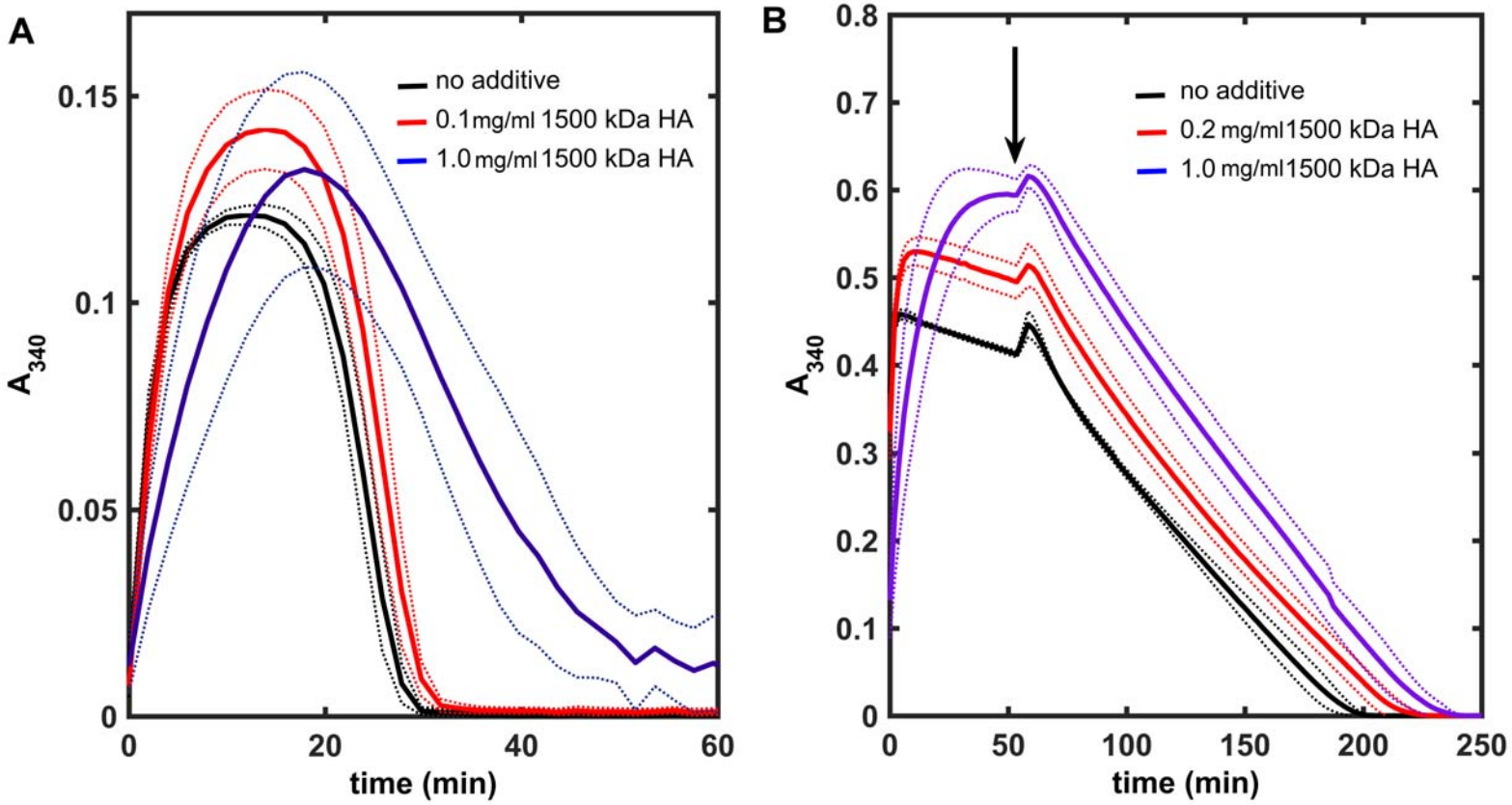
A
no additive
0.1 mg/ml 1500 kDa HA
1.0 mg/ml 1500 kDa HA
A340
time (min)
B
no additive
0.2 mg/ml 1500 kDa HA
1.0 mg/ml 1500 kDa HA
A340
time (min)

Figure 6